To appear in *Molecular Simulation*
Vol. 00, No. 00, Month 20XX, 1–12

Gibbs Ensemble Monte Carlo with Solvent Repacking: Phase Coexistence of Size-asymmetrical Binary Lennard-Jones Mixtures

Ziwei Guo and James T. Kindt*

Department of Chemistry, Emory University, Atlanta, Georgia 30322, USA

(*30 Jul 2017*)

Acknowledgements

This work was supported by the American Chemical Society Petroleum Research Fund under Grant 54642-ND6; Extreme Science and Engineering Discovery Environment (XSEDE), which is supported by National Science Foundation under Grant ACI-1548562; and the resources of the Cherry L. Emerson Center for Scientific Computation.

*Corresponding author. Email: jkindt@emory.edu

We describe a Monte Carlo method for simulation of vapor-liquid phase coexistence in size-asymmetrical Lennard-Jones (LJ) binary mixtures. The method incorporates the Solvent Repacking Monte Carlo (SRMC) approach, which offers efficient trial moves for the exchange of a large particle for several small particles, into the Gibbs Ensemble Monte Carlo (GEMC) method. SRMC yields a significant efficiency improvement in simulation of dilute large species mixtures at low temperature compared to the original Gibbs ensemble Monte Carlo method with identity exchange (IE) moves. Vapor-liquid phase diagrams are reported for LJ mixtures with a diameter ratio $\sigma_{SS} : \sigma_{LL}$ of 1:2 with well depth ratios $\epsilon_{SS} : \epsilon_{LL} = 1.2, 1.5$ and 2, producing spindle-type, azeotrope, and closed loop types of phase diagram, respectively.

Keywords: Lennard-Jones; Phase Coexistence; Gibbs ensemble Monte Carlo; Configuration bias Monte Carlo

1. Introduction

Phase diagrams of mixtures have intrigued the interest of scientific community for decades due to their importance in vapor-liquid distillation, supercritical extraction, and related industrial processes. Work on generating phase diagrams for mixtures of Lennard-Jones (LJ) fluids using various theoretical approaches has spanned several decades [1–9]. Size asymmetrical mixtures are studied by Gibbs Ensemble Monte Carlo (GEMC) [5, 10], Grand Canonical Ensemble Monte Carlo (GCMC) method [11, 12] or other simulation strategies [13–16]. Complete phase diagrams of binary LJ mixtures were reported by Hall et al. [15, 17] through Monte Carlo (MC) simulation and the Gibbs-Duhem integration method [18]. The first-order phase transition for binary mixtures has been calculated by the semigrand canonical ensemble method as well [19]. Calculations using the Redlich-Kwong equation of state show the phase diagrams for molecules of unequal sizes are topologically different from similar size molecules [20]. However, most research focuses on the LJ mixtures that have different well depth ϵ but with size ratios close to 1.

The development of the GEMC method by Panagiotopoulos [21] facilitated the study of phase coexistence of mixtures. Given the proper initial set up, the system can tune itself to produce a phase coexistence point. Due to these attributes of GEMC, it has broad applications in molecular simulations of phase equilibria [22, 23] including simulations of vapor-liquid coexistence in size-asymmetrical mixtures [5]. For asymmetrical mixtures, a trial move that can exchange the identity of different species is included in addition to the displacement move, volume exchange, and small particle swap moves. In practice, however, this GEMC method with identity exchange (IE) suffers from the low acceptance probabilities in simulations of dense systems at low temperature, especially when we want to insert a large particle into the space occupied by a large number of small particles.

The success of modified Gibbs ensemble Monte Carlo with IE moves depends on the existence of small particles that occupy cavities spacious enough to fit a large particle. These environments become vanishingly rare with increasing size ratio or with increasing density of the small particle in the liquid phase. The case of large size ratios and low small-particle density has been explored using innovative methods. Phase diagrams of highly size-asymmetric mixtures (with a 10:1 diameter ratio) in which the small component is not strongly attractive and is present at low (5%) volume fraction have been successfully studied [24, 25] through restricted GEMC simulation coupled with the highly efficient, rejection-free geometric cluster algorithm (GCA) [26]. The effectiveness of the GCA algorithm is limited, however, to a maximum small-particle volume fractions of about 0.34 [27]. A multicanonical staged insertion method has also been applied successfully to the same system [11]; it also becomes more expensive with increasing small-particle volume fraction, as it relies for its efficiency on rapid grand-canonical sampling of the small particles, and could face bottlenecks associated with cavity wetting/dewetting transitions of strongly attractive small particles as repulsions from the large particle are gradually turned off or on.

Here we will show that incorporation into GEMC of the Solvent Repacking Monte Carlo (SRMC) method [28], which offers the possibility of exchanging a variable number of small particles for a single large particle, can facilitate simulations in which the large species is effectively dissolved

in an excess of the small species. The SRMC method is based on the Configuration bias Monte Carlo (CBMC) algorithm [29], which was originally developed to perform efficient trial moves for segmented chain structures in dense environments. The basic idea for CBMC is to generate multiple possible positions for each segment, and only one is chosen based on their Boltzmann weights, biasing the positions of early segments toward lower-energy positions. When the trial steps reach the end of the segmented chain, the entire new chain configuration is accepted or rejected based on an acceptance probability that accounts for the biasing. CBMC has been commonly used in conjunction with the Gibbs Ensemble to improve acceptance probabilities for exchange of single, multisite particles between boxes [23].

In only a few cases has the CBMC approach been applied to generate configurations for multiple independent particles, because these cases can generally be treated efficiently using single-particle moves. In one case it was used to reposition small particles during large particle displacements in a size-asymmetric mixture [30]. Exchange of one particle with multiple particles of a different type has also been used in CBMC/GEMC simulations of mixtures of hard spheres with infinitely thin needles [31]. In a study by Wijmans et al. [32], polymer chains in solution could be exchanged very efficiently across GEMC boxes using a 1:1 exchange of polymer segments for solvent particles without changing the coordinates of either; CBMC sampling was used to select which solvent particles would be linked together into a chain. This relies on a similarity in interaction potentials between solvent and monomer particles. SRMC is distinguished by two innovations that are intended to address the challenge of generating a new arrangement of small particles to fill the cavity left by the large: the flexibility to exchange a variable number of small particles for a single large particle (depending on the microenvironment and the system state) and the use of an auxiliary potential to improve the chance of generating a well-packed solvent arrangement in the cavity. In the present system, we find that the auxiliary potential was not helpful, in contrast to its usefulness in a GCMC study of the fluid/ordered transition in bidisperse hard disk systems [28].

In the present work, we implement SRMC on three-dimensional Gibbs ensemble systems with a continuous interaction potential and study the phase behaviors for several mixtures. In cases where large particle has a greater attractive energy than the small particle, then this would describe a dilute solution of a non-volatile solute, which is not very interesting. Here, we consider the opposite case, $\epsilon_{SS} > \epsilon_{LL}$, where the pairwise attraction energy between small particles, ϵ_{SS}, is greater than that between large particles, ϵ_{LL}. As far as we know, the phase behavior of these LJ systems have not been simulated before. After confirming that our SRMC can reproduce the gas/liquid coexistence boundaries of LJ fluid mixtures previously reported in literature, we apply it to study the phase diagrams of LJ binary mixtures that have a 2:1 size ratios under different large/small particle ϵ ratios(1:1.2, 1:1.5 and 1:2) at a temperature of $0.75\epsilon_{SS}/k_B$. The efficiency analysis shows that the SRMC method is a useful complement to the simple IE move, allowing for reasonable success rates under conditions when the IE move fails, specifically at low liquid phase fractions of the large species and at low temperature.

2. Methods

In this section, the acceptance probabilities of Gibbs ensemble SRMC moves will be derived. A similar method in grand canonical ensemble is described in the paper of SRMC on hard disk mixtures [28].

2.1. *Gibbs ensemble SRMC algorithm*

In our new Gibbs ensemble Monte Carlo with solvent repacking, regular translation move and volume exchange move will be performed as well as the single particle swap for small species. To equilibrate the number of large particles across the two boxes, a large particle is exchanged for

zero, one, or (usually) more small particles as shown schematically in Fig 1.

The scheme of original solvent repacking move in hard-disk system is shown in Fig. 1 of [28]. First, a box for the large species to be removed from, one of the large particles it contains, and its new trial position in the other box are selected at random. If the liquid ("f" is used as indicator of liquid box in equations) box (defined as the box with the greater density, which in the present simulations is always unambiguous) is chosen, then a cavity is defined as the spherical volume within a distance of 1.38 σ_{SS}, which is justified in section *3.1.2* below, from the position of the large particle. If any small particles are present within this cavity (very unlikely due to repulsion from the large particle) the move is rejected. Otherwise, over a series of cycles indexed by i, which is also the index of the particle to be inserted, a number k of random positions that uniformly sample the space of the "cavity" will be generated. For each position j out of these k positions, the potential energy $u_{i,j}$ is calculated as the sum of the interactions with particles outside the cavity and the particles inserted in previous cycles ($i' < i$). In each cycle, one of the k positions is selected as the ith particle for the new trial set based on the probability of choosing position j',

$$P_{i,j'} = \frac{\exp(-\beta u_{i,j'})}{\sum_{j=1}^{k} \exp(-\beta u_{i,j})} \tag{1}$$

After selecting one as the ith particle in the new configuration set, we can proceed to the next cycles, increasing i by one. (In a previous study for hard disk system, an auxiliary potential was used to improve the acceptance probabilities of SRMC. However, as discussed in section *3.1.3*, an auxiliary potential is not used here because it was not found to improve the acceptance probabilities.)

To determine how many small species are inserted into the cavity during repacking, we define a weight associated with each state that has i particles inserted:

$$\omega_i = \frac{v_{cav}^i}{i!k^i} W_i \frac{N_{Sg}!}{(N_{Sg}-i)!} \frac{1}{V_g^i} \tag{2}$$

where v_{cav} is the volume of the cavity, N_{Sg} is the number of small species in vapor box, V_g is the volume of the vapor box. W is the Rosenbluth weight, which can be defined as

$$W_i = \prod_{i'=1}^{i} \sum_{j=1}^{k} \exp(-\beta u_{i',j}) \tag{3}$$

Cycles generating new particle positions are continued until W_i falls below a predetermined value (here set equal to 100). The maximum number that will then be considered, n_{max}, is set to be 1 fewer. The weight ω_i is used to select which value of $i' \in \{0, n_{max}\}$ will represent the number of particles to be actually inserted into the cavity. The i' small particles to be removed from the vapor box are selected at random. For reverse move that goes from a new configuration to an old one, if the sum of the Boltzmann weights is smaller than $W_{cut} = 100$ but we still have particles from the old configuration that need to be inserted, this entire SRMC move will be terminated immediately to preserve detailed balance.

The probabilities of generating a specific trial move to remove a large species from liquid box(f) to insert it into vapor box(g) is:

$$\alpha_{f\to g} = \frac{1}{N_{Lf}} \frac{\omega_{new}}{\sum_{i'=0}^{n_{max}} \omega_{new,i'}} \frac{n_{cav}!}{v_{cav}^{n_{cav}}} \left(\prod_{i=1}^{n_{cav}} k_i P_{i,j',new}\right) \frac{1}{V_g} \frac{(N_{Sg}-n_{cav})!}{N_{Sg}!} n_{cav}! \tag{4}$$

For its reversal, to transfer that large species from vapor box to liquid box is:

$$\alpha_{g\to f} = \frac{1}{V_f}\frac{1}{N_{Lg}+1}\frac{n_{cav}!}{V_g^{n_{cav}}} \tag{5}$$

where N_{Lf} is the number of large species in liquid box, N_{Lg} is the number of large species in vapor box, V_f is the volume of the the liquid box. An acceptance probability satisfying detailed balance can be derived as:

$$\begin{aligned} acc &= \frac{\alpha_{g\to f}}{\alpha_{f\to g}}\exp[-\beta(U_{f,new}-U_{f,old}+U_{g,new}-U_{g,old})] \\ &= \frac{V_g N_{Lf}\sum_{i'=0}^{n_{max}}\omega_{new,i'}}{V_f(N_{Lg}+1)}\frac{\exp(-\beta U_{Lg,new})}{\exp(-\beta U_{Lf,old})\exp(-\beta U_{Sg,old})} \end{aligned} \tag{6}$$

where U is the potential energy of liquid box or vapor box in new configuration (after transferring a large species from liquid box to vapor box) or old configuration.

If the vapor box is selected for removal of large species, a random position for the cavity will be generated to insert the large species in the liquid box. Meanwhile, a number i' of small species in that cavity region will be moved to randomly selected positions in the vapor box. The probability of the reverse move, which is the move to insert i' small species back to the cavity in the liquid box by SRMC, will be calculated by sampling of "dummy" positions to calculate the appropriate Rosenbluth weights W_i. The acceptance rule can be derived using the same method as removing a large species from the vapor box:

$$\begin{aligned} acc &= \frac{\alpha_{f\to g}}{\alpha_{g\to f}}\exp[-\beta(U_{f,new}-U_{f,old}+U_{g,new}-U_{g,old})] \\ &= \frac{V_f N_{Lg}}{V_g(N_{Lf}+1)\sum_{i'=0}^{n_{max}}\omega_{old,i'}}\frac{\exp(-\beta U_{Lf,new})\exp(-\beta U_{Sg,new})}{\exp(-\beta U_{Lg,old})} \end{aligned} \tag{7}$$

2.2. *Implementation details*

Pairs of particles interact via the Lennard-Jones potential:

$$\Phi_{ij}(r) = 4\epsilon_{ij}[(\frac{\sigma_{ij}}{r})^{12}-(\frac{\sigma_{ij}}{r})^{6}] \tag{8}$$

The following mixing rule is applied when calculate the cross term of potential energy: $\sigma_{SL} = (\sigma_{SS}+\sigma_{LL})/2$, $\epsilon_{SL} = \sqrt{\epsilon_{SS}\epsilon_{LL}}$. The shifted potential Φ is used in all simulations:

$$\Phi_\alpha(r) = \frac{1}{r^\alpha} - \frac{A}{3}(r-r_{shift})^3 - \frac{B}{4}(r-r_{shift})^4 - C; (r_{shift}\le r\le r_{cut}) \tag{9a}$$

$$\Phi_\alpha(r) = \frac{1}{r^\alpha} - C; (r\le r_{shift}) \tag{9b}$$

where the parameters A,B and C can be calculated as:

$$A = \frac{\alpha\{(\alpha+1)r_{shift} - (\alpha+4)r_{cut}\}}{r_{cut}^{(\alpha+2)}(r_{cut} - r_{shift})^2} \tag{10a}$$

$$B = \frac{\alpha\{(\alpha+1)r_{shift} - (\alpha+3)r_{cut}\}}{r_{cut}^{(\alpha+2)}(r_{cut} - r_{shift})^3} \tag{10b}$$

$$C = \frac{1}{r_{cut}^{\alpha}} - \frac{A}{3}(r_{cut} - r_{shift})^3 - \frac{B}{4}(r_{cut} - r_{shift})^4 \tag{10c}$$

where α represents the power of the respective LJ terms (6 or 12). Shifted potentials enable the potential and force to continuously and smoothly decay to zero between $r_{shift} = 3\sigma$ and the cut-off distance $r_{cut} = 4\sigma$, and were useful for cross-checking our Monte Carlo codes with results from molecular dynamics simulations (not shown). In our study, different r_{shift} and r_{cut} are used for three interactions (two interactions among small and large, one cross term of interaction). We employed periodic boundary conditions with long-range corrections to approximate infinite thermodynamic properties of systems with finite size systems, which will give us the phase diagrams and thermodynamics properties reflecting a true LJ fluid. The following functions for pressure and potential energy are added to the mean values used or extracted from simulations as mean-field corrections for the long-ranged contributions of the LJ potential that are neglected in simulations due to truncation [33]:

$$\begin{aligned} p_{lrc} = &\frac{32}{9}\pi\rho_S^2(r_{cut}(SS)^{-9} - \frac{3}{2}r_{cut}(SS)^{-3}) \\ &+ \frac{32}{9}\pi\rho_L^2(r_{cut}(LL)^{-9} - \frac{3}{2}r_{cut}(LL)^{-3}) \\ &+ \frac{64}{9}\pi\rho_S\rho_L(r_{cut}(SL)^{-9} - \frac{3}{2}r_{cut}(SL)^{-3}) \end{aligned} \tag{11}$$

$$\begin{aligned} u_{lrc} = &\frac{8}{9}\pi N_S\rho_S(r_{cut}(SS)^{-9} - 3r_{cut}(SS)^{-3}) \\ &+ \frac{8}{9}\pi N_L\rho_L(r_{cut}(LL)^{-9} - 3r_{cut}(LL)^{-3}) \\ &+ \frac{16}{9}\pi N_S\rho_L(r_{cut}(SL)^{-9} - 3r_{cut}(SL)^{-3}) \end{aligned} \tag{12}$$

The equilibration and production periods each consisted of at least 2×10^5 MC moves. In our SRMC Gibbs ensemble simulations, the type of MC move was selected randomly according to the following ratios: 1(consisted of 1000 single particle swap cycles):5(SRMC):1(volume exchange). In Gibbs ensemble simulations with IE used to make the performance comparison, the type of MC moves has a ratio: 1(consisted of 1000 single particle swap cycles):5(consisted of 600 IE moves):1(volume exchange). In both cases, each move was followed by 100 translation moves for small and large species, respectively. The only difference is we replaced 1 SRMC move with 600 IE moves, because we found the CPU time for one SRMC is approximately equal to 600 IE moves. The diameters of the cavities are fixed at $2.76\sigma_{SS}$. Multiple insertions ($k = 500$) are used in SRMC moves. The maximum distance for translation move is set to $0.05\sigma_{SS}$ and $0.01\sigma_{SS}$ for

small and large species, respectively. The maximum volume change is set to $0.1\sigma_{SS}^3$. Error bars in the following phase diagrams are generated by block averaging.

3. Results and Discussion

In this section, we first present the different strategies used to optimize our new SRMC method. Then, the vapor-liquid phase transition of LJ fluid mixtures is demonstrated and compared with literature results to validate our SRMC method. The applications to binary mixtures under different ratios of ϵ at a low temperature is described and performance analysis is reported to show capability and efficiency enhancement of SRMC in simulations of dilute large species fluids.

3.1. *Optimization of SRMC*

In order to get the best performance, we optimized our SRMC from the following approaches: the number of random trial position k, cavity size, and use of auxiliary bias potential function.

3.1.1. Optimization of k

The number of random trial positions k affects both acceptance probability and performance of the SRMC method. A low k will save computational effort but decrease the acceptance rate. Therefore the objective is to find a balance between these two that gives the best performance. To quantify the performance, we define a parameter Suf/hr to characterize the successful large particle swap moves per CPU hour. Fig 2 shows the acceptance probabilities and Suf/hr at different k. The best performance can be obtained in the range $10 < k < 25$. In this work we used a higher value, $k = 500$, which we anticipate would be more appropriate for replacement of even larger particles.

3.1.2. Optimization of cavity size

Fig 3 shows the effect of cavity size on acceptance probabilities and performance. Best values can be obtained at cavity radius equal to $1.38\sigma_{SS}$. Due to the 2:1 size ratio, σ_{SL} equals $1.5\sigma_{SS}$. The best cavity radius is therefore slightly smaller than σ_{SL}, so small particle trial positions will lie inside the solvent shell of the large particles.

3.1.3. Use of auxiliary bias potential function

Auxiliary bias potential function can be used to improve acceptance probabilities by incorporating many-body effects into the selection of particle positions, accounting in a mean field way for the influence of particles not yet inserted into the cavity. In previous work using the SRMC method, use of the radial distribution function (RDF) as an auxiliary potential ($u_{bias} = \ln g(r)/\beta$) increased the acceptance rate significantly for large size ratio hard disk mixtures [28]. For the 3D LJ mixtures we generated a fit to the difference between LJ potential with RDF using a sum of Gaussian functions (Fig 4). To then determine whether an auxiliary potential improved the acceptance probability of the SRMC method, we introduced a bias potential function $\exp(-\beta u_{bias}) = \exp(-\beta u_{bare}) + \lambda(g(r) - \exp(-\beta u_{bare}))$, where the contribution from the RDF bias potential can be scaled by a parameter λ. By tuning λ from 0 to 1, we can gradually switch our bias potential from full bare potential to full RDF. However, in contrast to 2D hard disk system, using the RDF to bias selection of particle positions does not increase the acceptance probability (Fig 5). It is possible that the RDF does not give a good representation of interparticle distances in the environment of the average cavity left by a large particle, or that the cavities are too small for incorporation of these effects to be helpful. We tried auxiliary bias potential function at a larger size ratio system ($\sigma_{LL} : \sigma_{SS} = 2.5{:}1$), but similarly found no increase in acceptance probability.

3.2. *Phase diagram of binary mixtures*

The SRMC is applied to studying the phase behavior of LJ binary mixtures with diameter ratios $\sigma_{LL} : \sigma_{SS} = 2 : 1$. To validate the SRMC-GEMC method, we first applied it to a system with ϵ ratios: $\epsilon_{LL} : \epsilon_{SS} = 4 : 1$ at $T^* = 1.0\epsilon_{SS}/k_B$. Fig 6 shows the comparison between our SRMC and original GEMC with IE. Our simulated data has a good agreement with the GEMC data reported in literature [5], which validates our method in the simulation of LJ mixtures. Next, the phase diagrams of 3 LJ systems with size ratio 2:1 at $T^* = 0.75\epsilon_{SS}/k_B$ are shown in Fig 7, 8 and 9. $x(L)$, $y(L)$ denotes the the mole fraction of large species in liquid phase and vapor phase, respectively. As ϵ_{LL} is decreased, there is a shift in vapor phase enrichment from small species to large species across different systems, listed in Table 1. It can be explained by the balance between ϵ and number of neighbors for certain particle. When the attractive energies of both species are similar (as in 1:1.2 ratio, Fig 7), large particles are preferentially retained in the liquid phase they have more neighbors to attract them, even if the average energy of attraction is slightly lower. After decreasing the ϵ_{LL} (Fig 8, and 9), the stronger attractions of small species becomes more important than their smaller number of neighbors, which make large species more likely to escape to the vapor phase. The phase diagram of ϵ ratio 1:1.5 (Fig 8) shows an azeotrope point at large species fraction near 0.75. When large species fraction is smaller than 0.75, large particles are over-represented in the vapor phase, while in high large species concentration mixtures($x(L) > 0.75$), the small species is a little bit enriched in vapor phase. Trends in coordination numbers of large and small species(Table 1) might shed light on this behavior. The crossover seems to coincide with the transition from small particles having mostly small neighbors, allowing for the strongest neighbor bonding in the system, to having mostly large neighbors, where the number of large neighbors surrounding a small particle is limited by steric factors. For the ϵ ratio 1:2, the phase diagrams demonstrate a closed circle because the temperature is higher than the critical point of the large species.

Fig 10 shows a partial phase diagram for size ratio $\sigma_{LL} : \sigma_{SS} = 2.5 : 1$ with $\epsilon_{LL} : \epsilon_{SS} = 1 : 1.5$, which demonstrate the applicability of SRMC to a larger size ratio. However, increasing the size ratio to $3 : 1$ resulted in a too low acceptance probability that prevented us from achieving equilibrium in a reasonable simulation time.

3.3. *Performance Comparison between SRMC with identity exchange swap method*

Table 2 compares the performances (Suf/hr), measured in successful large particle swaps per hour, of SRMC and the IE method in Gibbs ensemble at different large species mole fractions($x(L)$) in the liquid phase. We tracked the number fluctuations of large particles achieved using different methods versus CPU time. Clearly, SRMC can swap the large species more frequently than simple IE move (as shown in Fig 11), which allows few or no successful swaps in a dilute large species environment. The reason why the original IE method failed in this regime is due to the increasing difficulty finding the free volume to fit a large particle size increase in IE in a very dense phase consisting of a large amount of small species. In contrast, SRMC can swap large species into dense environment in exchange for multiple small particles, allowing access the phase properties of dilute large species mixtures. We note that the IE method is more efficient when the large species is not dilute. We plot Suf/hr versus the large species fraction in liquid phase to compare the performances of the two methods(Fig 12, 13, and 14), and see a crossover from conditions where SRMC is more efficient to where single IE is preferable as the mole fraction of large particles increases. The crossover takes place near a mole fraction $x(L)$ of 50% at ϵ ratios 1:1.2 and 1:1.5, but at much lower fraction for the ϵ ratio 1:2 case. In that case, the increase in large particle content brings the coexisting phases near a critical point, with the density of the liquid phase falling while the density of the gas phase rises. The decrease in density of the liquid phase helps the simple IE move while the increase in density of the gas phase hurts the SRMC move, which in the present implementation involves multiple unbiased insertions of the small particles into this dense gas. Incorporating multiple trial

positions for insertion into the gas phase could improve performance under these circumstances.

The performance measures are low in absolute terms for a combination of reasons. Our code will achieve 203,000 successful simple small particle swaps per hour on an Intel Xeon E5-2680v3 processor core of the Comet cluster at the San Diego Supercomputer center at $T^* = 1.0$. This rate decreases to 10,800 at $T^* = 0.75$ due to the increased density and decreased temperature. These values reflect the availability of voids, thermally generated within the liquid phase, whose volume is sufficient to insert a small particle. As evident from the values shown in Fig 12-14, IE moves in a mixture with a diameter ratio of 2:1 are further suppressed by one or more orders of magnitude (depending on mixture composition) because they require a free volume of approximately the difference between the large and small particle volumes (i.e. seven times the small particle volume). The solvent repacking approach can avoid this problem by exchanging a large particle for a cluster of solvent with equal volume. The trade-off in computational expense, however, is the challenge of finding a compact, low-energy packing arrangement for multiple solvent particles in the large particle's vacated cavity, requiring many trial positions to be generated per move.

4. Conclusions

In summary, we implemented the SRMC method for the study of vapor-liquid coexistence of size-asymmetrical binary LJ mixtures. The SRMC can overcome the low acceptance probabilities in traditional GEMC simulations of dilute solute mixtures at low temperature, which offer the exchange of one large particle for several small particles. We have applied our SRMC to phase transition studies of three binary size-asymmetric LJ mixtures with different ϵ ratios, and seen a range of vapor-liquid phase transition behaviors. Further refinements of the SRMC method may enable its application to thermodynamic and phase behavior of more complex fluid systems, including aqueous solutions.

Acknowledgements

Acknowledgment is made to the Donors of the American Chemical Society Petroleum Research Fund for support of this research through grant 54642-ND6. This work used the Extreme Science and Engineering Discovery Environment (XSEDE), which is supported by National Science Foundation grant number ACI-1548562, and the resources of the Cherry L. Emerson Center for Scientific Computation.

References

[1] Nicolas J, Gubbins K, Streett W, et al. Equation of state for the Lennard-Jones fluid. Molecular Physics. 1979;37:1429–1454.
[2] Rowlinson J. Liquids and Liquid Mixtures. London: Butterworth Scientific; 1982.
[3] Mazur V, Boshkov L, Murakhovsky V. Global phase behaviour of binary mixtures of Lennard-Jones molecules. Physics Letters A. 1984;104:415–418.
[4] Johnson JK, Zollweg JA, Gubbins KE. The Lennard-Jones equation of state revisited. Molecular Physics. 1993;78:591–618.
[5] Georgoulaki AM, Tassios DP, Panagiotopoulos AZ, et al. Phase equilibria of binary Lennard-Jones mixtures: simulation and Van Der Waals l-fluid theory. Fluid Phase Equilibria. 1994;100:153–170.
[6] Mecke M, Müller A, Winkelmann J, et al. An accurate Van Der Waals-type equation of state for the Lennard-Jones fluid. International Journal of Thermophysics. 1996;17:391–404.
[7] Lin ST, Blanco M, Goddard III WA. The two-phase model for calculating thermodynamic properties

of liquids from molecular dynamics: Validation for the phase diagram of Lennard-Jones fluids. The Journal of Chemical Physics. 2003;119:11792–11805.
[8] Pastore G, Santin R, Taraphder S, et al. Fluid-phase diagrams of binary mixtures from constant pressure integral equations. The Journal of Chemical Physics. 2005;122:181104.
[9] Stringari P, Campestrini M. Application of the SLV-EoS for representing phase equilibria of binary Lennard-Jones mixtures including solid phases. Fluid Phase Equilibria. 2013;358:68–77.
[10] Potoff JJ, Panagiotopoulos AZ. Critical point and phase behavior of the pure fluid and a Lennard-Jones mixture. The Journal of Chemical Physics. 1998;109:10914–10920.
[11] Ashton DJ, Wilding NB. Grand canonical simulation of phase behaviour in highly size-asymmetrical binary fluids. Molecular Physics. 2011;109:999–1007.
[12] Kumar V, Errington JR. Monte Carlo simulation strategies to compute interfacial and bulk properties of binary fluid mixtures. The Journal of Chemical Physics. 2013;138:174112.
[13] Fincham D, Quirke N, Tildesley D. Computer simulation of molecular liquid mixtures. I. A diatomic Lennard-Jones model mixture for CO2/C2H6. The Journal of Chemical Physics. 1986;84:4535–4546.
[14] Lamm MH, Hall CK. Molecular simulation of complete phase diagrams for binary mixtures. AIChE Journal. 2001;47:1664–1675.
[15] Lamm MH, Hall CK. Equilibria between solid, liquid, and vapor phases in binary Lennard-Jones mixtures. Fluid Phase Equilibria. 2002;194:197–206.
[16] Watanabe H, Ito N, Hu CK. Phase diagram and universality of the Lennard-Jones gas-liquid system. The Journal of Chemical Physics. 2012;136:204102.
[17] Galbraith AL, Hall C. Vapor-liquid phase equilibria for mixtures containing diatomic Lennard-Jones molecules. Fluid Phase Equilibria. 2006;241:175–185.
[18] Kofke DA. Gibbs-Duhem integration: a new method for direct evaluation of phase coexistence by molecular simulation. Molecular Physics. 1993;78:1331–1336.
[19] Tang Y. A new method of semigrand canonical ensemble to calculate first-order phase transitions for binary mixtures. The Journal of Chemical Physics. 2012;136:034505.
[20] Deiters UK, Pegg IL. Systematic investigation of the phase behavior in binary fluid mixtures. I. Calculations based on the Redlich-Kwong equation of state. The Journal of Chemical Physics. 1989;90:6632–6641.
[21] Panagiotopoulos A. Exact calculations of fluid-phase equilibria by Monte Carlo simulation in a new statistical ensemble. International Journal of Thermophysics. 1989;10:447–457.
[22] Chen B, Siepmann JI, Klein ML. Direct Gibbs Ensemble Monte Carlo simulations for solid-vapor phase equilibria: Applications to Lennard-Jonesium and Carbon Dioxide. The Journal of Physical Chemistry B. 2001;105:9840–9848.
[23] Bai P, Siepmann JI. Assessment and optimization of configurational-bias Monte Carlo particle swap strategies for simulations of water in the Gibbs ensemble. Journal of Chemical Theory and Computation. 2017;13:431–440.
[24] Liu J, Wilding NB, Luijten E. Simulation of phase transitions in highly asymmetric fluid mixtures. Physical Review Letters. 2006;97:115705.
[25] Ashton DJ, Liu J, Luijten E, et al. Monte Carlo cluster algorithm for fluid phase transitions in highly size-asymmetrical binary mixtures. The Journal of Chemical Physics. 2010;133:194102.
[26] Liu J, Luijten E. Rejection-free geometric cluster algorithm for complex fluids. Physical Review Letters. 2004;92:035504.
[27] Liu J, Luijten E. Generalized geometric cluster algorithm for fluid simulation. Physical Review E. 2005; 71:066701.
[28] Kindt JT. Grand canonical Monte Carlo using Solvent Repacking: Application to phase behavior of hard disk mixtures. The Journal of Chemical Physics. 2015;143:124109.
[29] Siepmann JI, Frenkel D. Configurational bias Monte Carlo: a new sampling scheme for flexible chains. Molecular Physics. 1992;75:59–70.
[30] Biben T, Bladon P, Frenkel D. Depletion effects in binary hard-sphere fluids. Journal of Physics: Condensed Matter. 1996;8:10799.
[31] Bolhuis P, Frenkel D. Numerical study of the phase diagram of a mixture of spherical and rodlike colloids. The Journal of Chemical Physics. 1994;101:9869–9875.
[32] Allen MP, Tildesley DJ. Computer simulation of liquids. Oxford University Press; 1989.

Table 1. Number of neighbors at different large species fractions for system $\sigma_{LL} : \sigma_{SS} = 2 : 1$, $\epsilon_{LL} : \epsilon_{SS} = 1 : 1.5$, $T^* = 0.75$

$x(L)$	nLL[a]	nSS	nLS	nSL
0		12.78		
0.0135	0.95	12.05	24.05	0.33
0.0576	3.14	10.47	18.62	1.14
0.3167	7.47	5.06	8.15	3.77
0.5779	10.70	3.10	4.38	6.01
0.7489	10.67	1.62	2.30	6.82
0.8321	10.64	0.78	1.35	6.70
0.9161	10.51	0.24	0.62	6.75
1	10.36			

[a]The first letter denotes the center particle while the second letter denotes its neighbors. The cut-off for a neighbor is defined at $1.5\sigma_{SS}$ for nSS, $3.1\sigma_{SS}$ for nLL, $2.1\sigma_{SS}$ for nLS and nSL, respectively.

Table 2. Performance comparison (as rate of successful large-particle exchanges per CPU-hour, Suf/hr) of GEMC-IE and SRMC in dilute large species mixtures

$\sigma_{LL} : \sigma_{SS}$	$\epsilon_{LL} : \epsilon_{SS}$	$x(L)$	Suf/hr(GEMC-IE)	Suf/hr(SRMC)
2:1	1:1.2	0.0301	0	35.04
2:1	1:1.2	0.0617	0.07	54.87
2:1	1:1.2	0.0970	0.63	80.30
2:1	1:1.2	0.1277	2.22	82.70
2:1	1:1.5	0.0282	0.05	38.01
2:1	1:1.5	0.0576	0.41	63.11
2:1	1:1.5	0.0888	3.78	89.39
2:1	1:1.5	0.1233	16.66	128.27
2:1	1:2	0.0004	0	0.90
2:1	1:2	0.0066	0	0.71
2:1	1:2	0.0109	0	0.62
2:1	1:2	0.0205	0	0.26

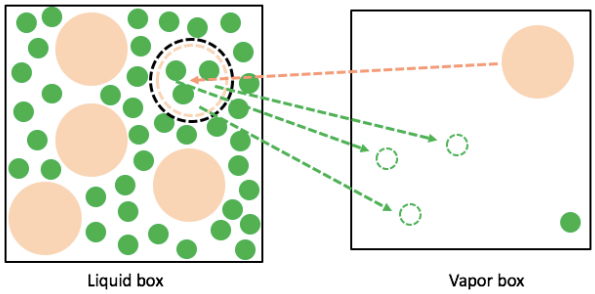

Figure 1. Scheme of SRMC in Gibbs ensemble: Insertion of a large particle in liquid box by SRMC, while using simple insertions to add multiple small species in vapor box.

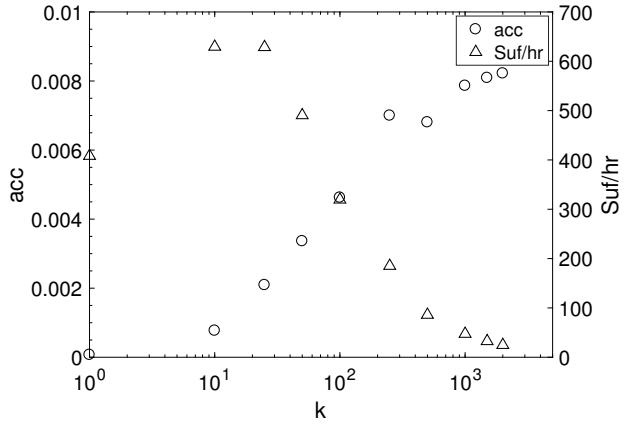

Figure 2. Acceptance probability(acc) and performance(Suf/hr) of SRMC method at different numbers of random trial positions k.

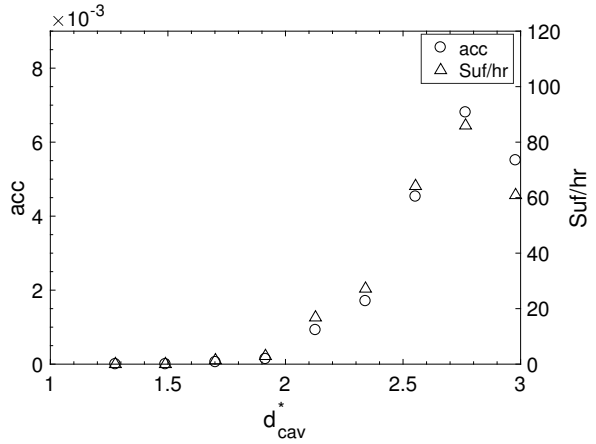

Figure 3. Acceptance probability(acc) and performance(Suf/hr) of SRMC method at different cavity diameter d^*_{cav}(reduced unit is used here: $d^*_{cav} = d_{cav}/\sigma_{SS}$).

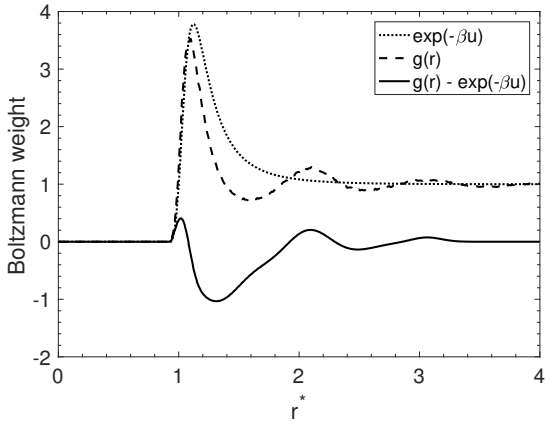

Figure 4. RDF of small species, Boltzmann weight of LJ potential, and difference (fitted by sum of Gaussian).

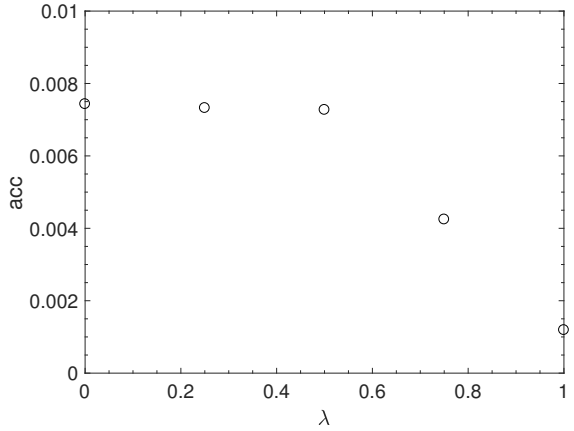

Figure 5. Acceptance probability(*acc*) of SRMC method incorporating auxiliary bias potential scaled by factor λ.

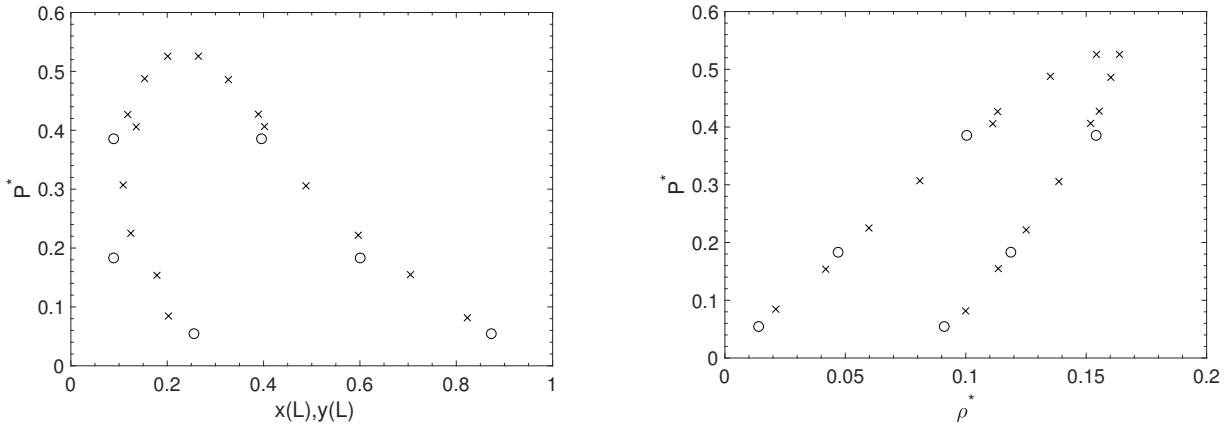

(a) (b)

Figure 6. Reduced pressure vs. mole fraction (a) and reduced density (b) for system ($\sigma_{LL} : \sigma_{SS} = 2 : 1$, $\epsilon_{LL} : \epsilon_{SS} = 4 : 1$, $T^* = 1.0$): ◯, SRMC results; ×, literature data [5].

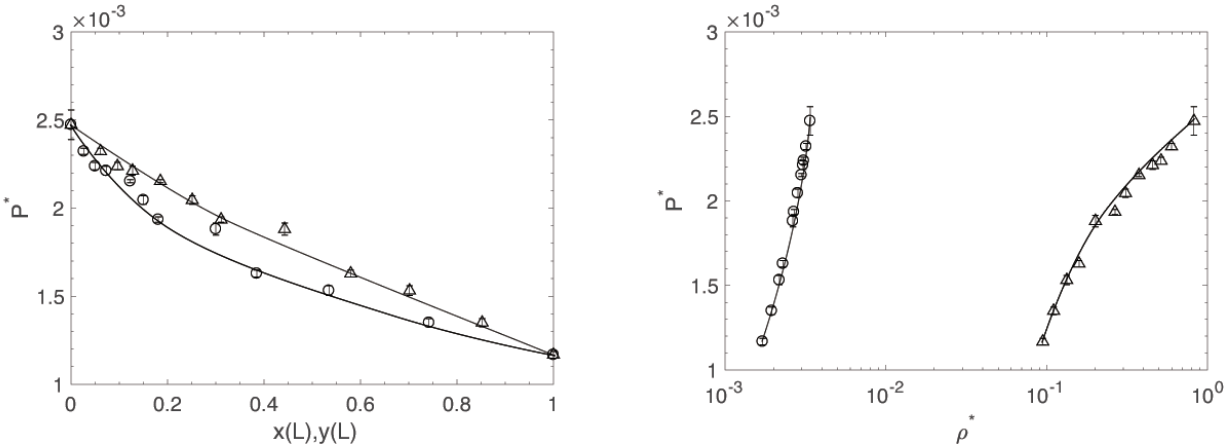

(a) (b)

Figure 7. Reduced pressure vs. mole fraction (a) and reduced density (b) for system ($\sigma_{LL} : \sigma_{SS} = 2 : 1$, $\epsilon_{LL} : \epsilon_{SS} = 1 : 1.2$, $T^* = 0.75$). Lines on the phase boundaries are drawn only as a guide to the eye. △ indicates the liquid phase boundary, and ◯ indicates the vapor phase boundary.

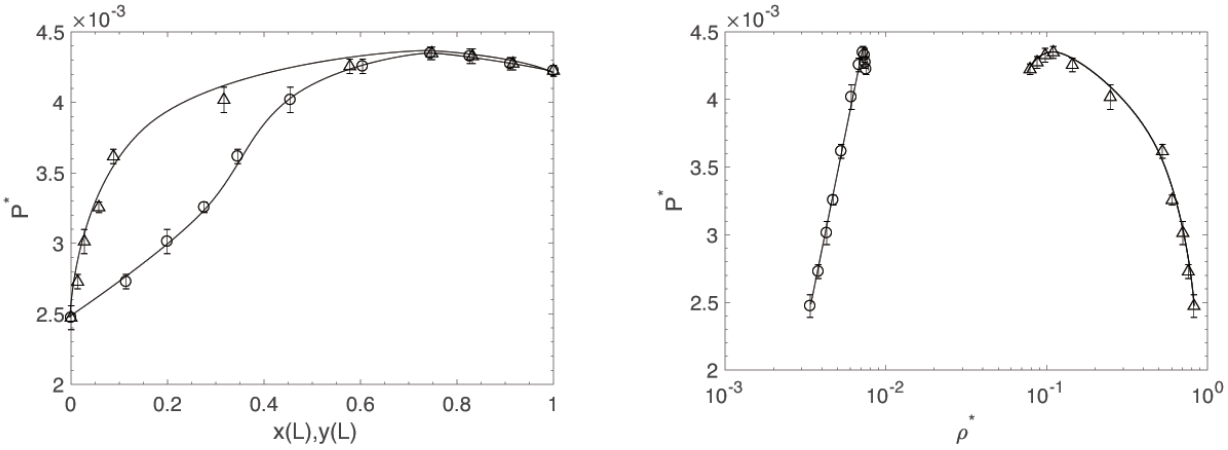

(a) (b)

Figure 8. Reduced pressure vs. mole fraction (a) and reduced density (b) for system ($\sigma_{LL} : \sigma_{SS} = 2 : 1$, $\epsilon_{LL} : \epsilon_{SS} = 1 : 1.5$, $T^* = 0.75$). Lines on the phase boundaries are drawn only as a guide to the eye. △ indicates the liquid phase boundary, and ◯ indicates the vapor phase boundary.

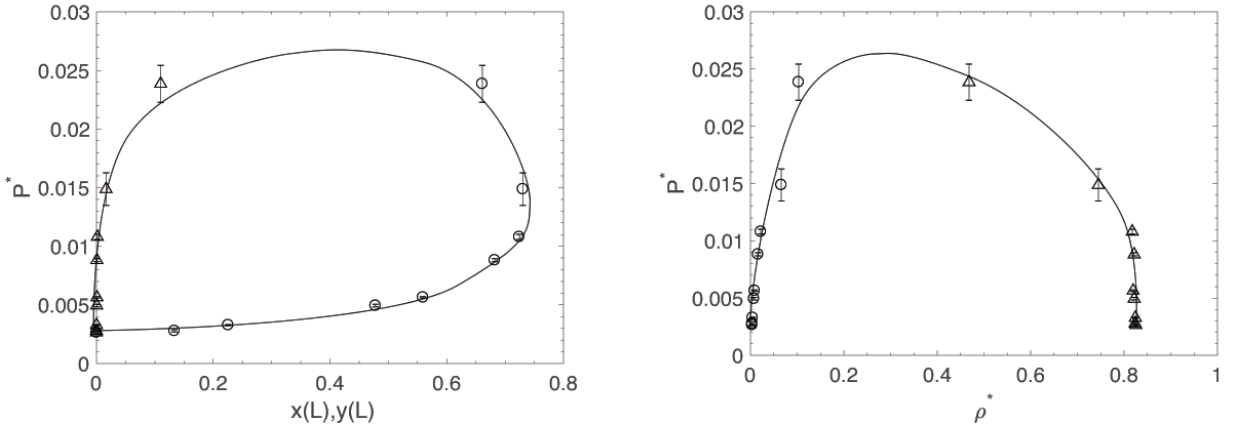

(a) (b)

Figure 9. Reduced pressure vs. mole fraction (a) and reduced density (b) for system ($\sigma_{LL} : \sigma_{SS} = 2 : 1$, $\epsilon_{LL} : \epsilon_{SS} = 1 : 2$, $T^* = 0.75$). Lines on the phase boundaries are drawn only as a guide to the eye. △ indicates the liquid phase boundary, and ◯ indicates the vapor phase boundary.

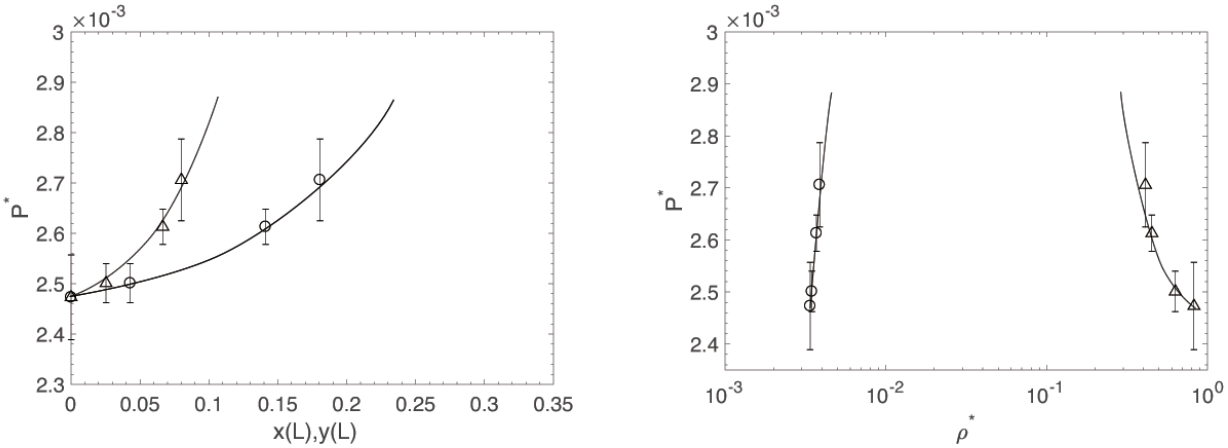

(a) (b)

Figure 10. Reduced pressure vs. mole fraction (a) and reduced density (b) for system ($\sigma_{LL} : \sigma_{SS} = 2.5 : 1$, $\epsilon_{LL} : \epsilon_{SS} = 1 : 1.5$, $T^* = 0.75$). Lines on the phase boundaries are drawn only as a guide to the eye. △ indicates the liquid phase boundary, and ◯ indicates the vapor phase boundary. Only dilute large species part is shown in this diagram.

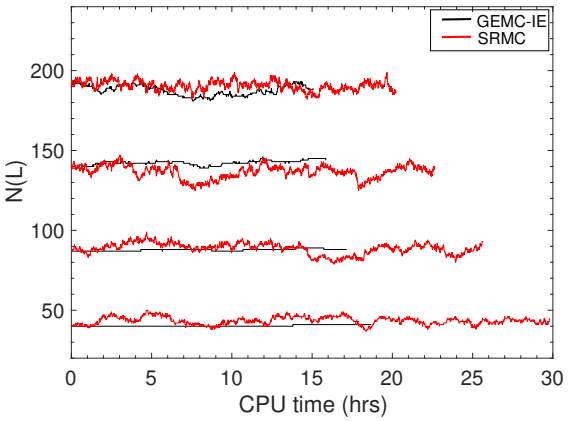

Figure 11. Number of large species in liquid phase simulated by GEMC-IE and SRMC for system ($\sigma_{LL} : \sigma_{SS} = 2 : 1$, $\epsilon_{LL} : \epsilon_{SS} = 1 : 1.5$, $T^* = 0.75$) at four total system compositions.

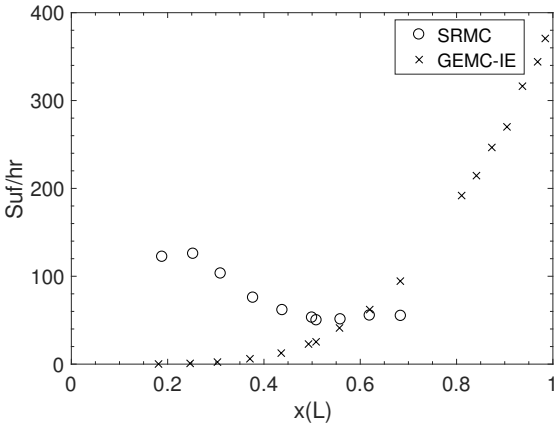

Figure 12. Performance of GEMC-IE and SRMC at different large species fractions (liquid phase) for system ($\sigma_{LL} : \sigma_{SS} = 2 : 1$, $\epsilon_{LL} : \epsilon_{SS} = 1 : 1.2$, $T^* = 0.75$).

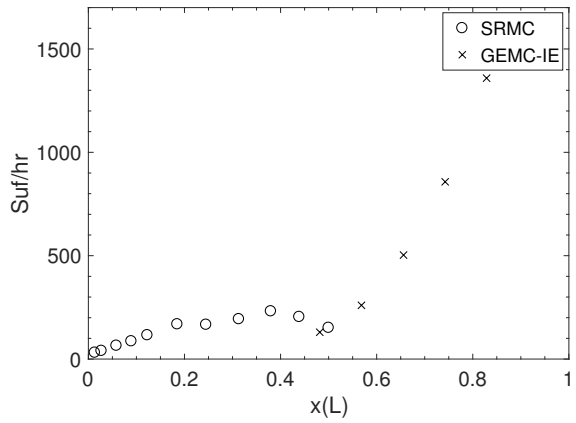

Figure 13. Performance of GEMC-IE and SRMC at different large species fractions (liquid phase) for system ($\sigma_{LL} : \sigma_{SS} = 2 : 1$, $\epsilon_{LL} : \epsilon_{SS} = 1 : 1.5$, $T^* = 0.75$).

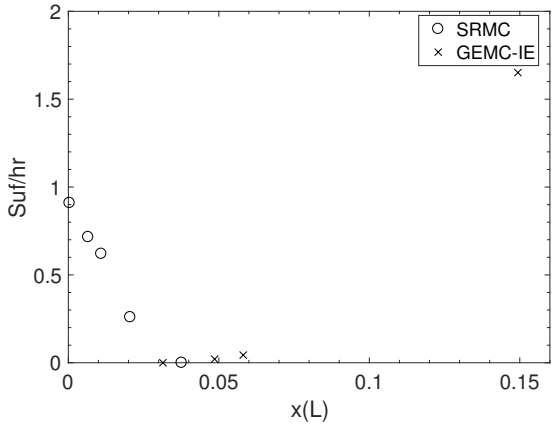

Figure 14. Performance of GEMC-IE and SRMC at different large species fractions (liquid phase) for system ($\sigma_{LL} : \sigma_{SS} = 2 : 1$, $\epsilon_{LL} : \epsilon_{SS} = 1 : 2$, $T^* = 0.75$).